Critical state soil models for dynamic analysis

Maxim Millen

30th September 2021

Soil constitutive models

A set of equations describing the material response to loading in terms of stress–strain relations.

Adaptable to many problems…

1D response

- G-γ, ξ-γ
- r_u-n_{cycles}

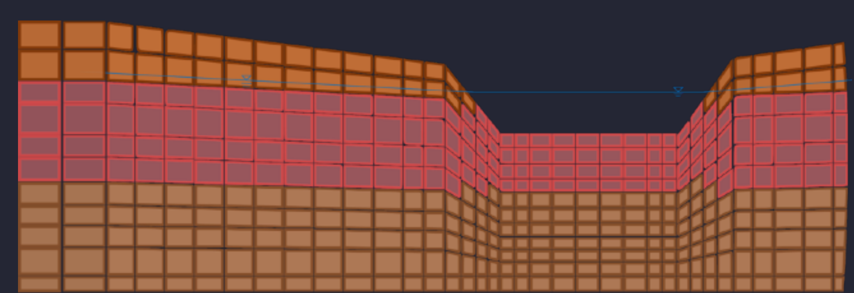

Lateral spreading

- Post-liq response
- Static stress response

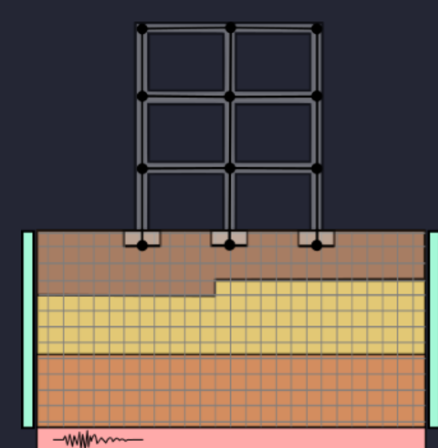

SFSI

- Small-strain response
- Strength capacity
- Cyclic strain development

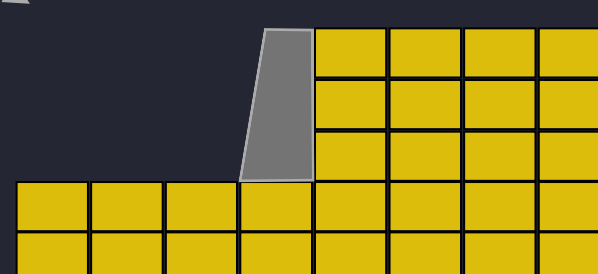

Retaining wall

- Horizontal pressure
-

But each problem has different calibration focus!

Develop expressions for foundation behaviour

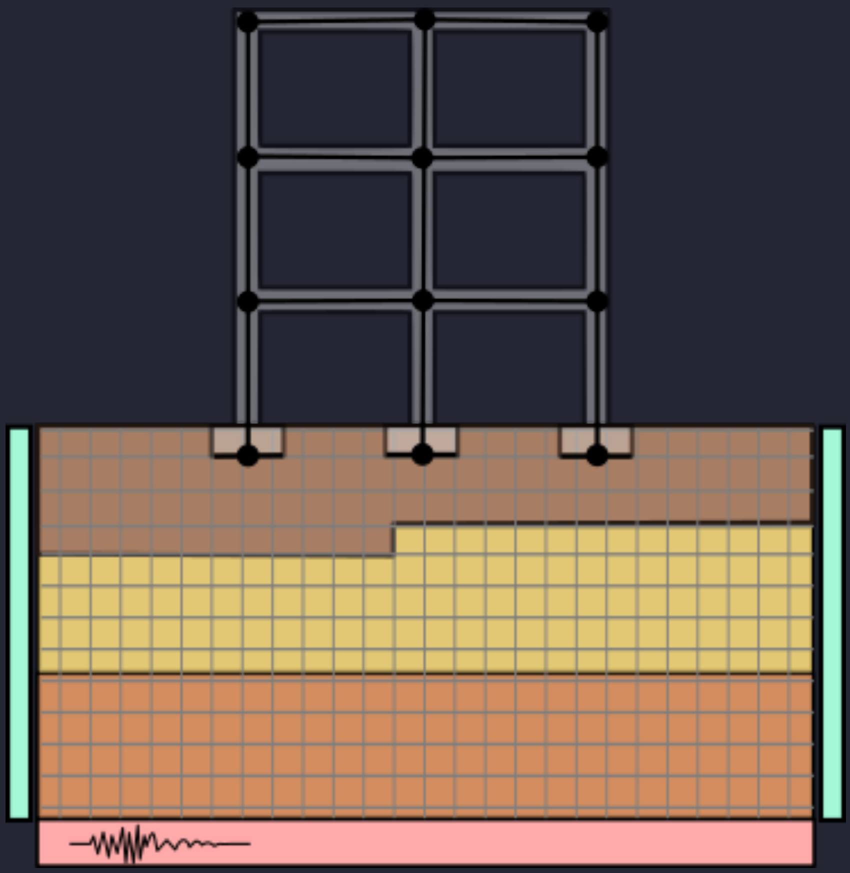

- Quasi-elastic average shear modulus for different DOFs for different FOS
- Rotation vs settlement and residual tilt

- Footing-to-footing interaction
- Heterogeneous soil response

Elastoplastic Constitutive models

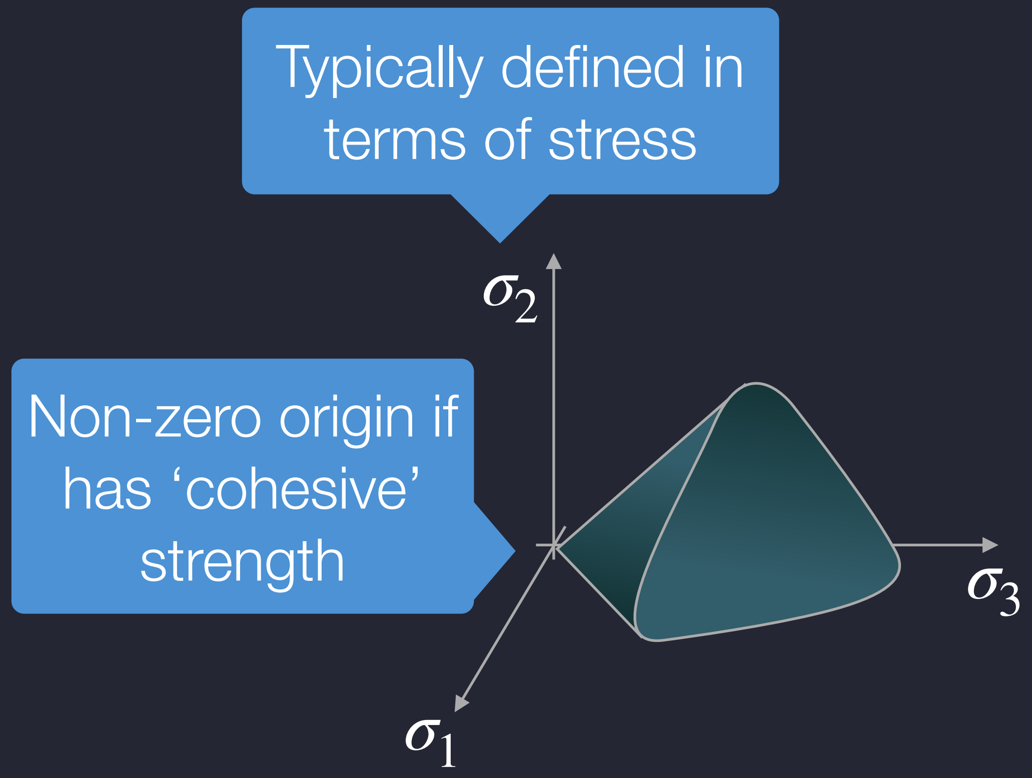

Components of elastoplastic models:

- **Elastic model**: Linear stress-strain behaviour
- **Hardening/softening rules:** Controls size and position of yield/loading surface based on plastic strain
  - Isotropic: Expansion/contraction
  - Kinematic: Translation
- **Flow rule** (Plastic potential function and Mapping rule): Direction and magnitude of plastic strain:
  - Associative: In direction of load vector
  - Non-associative: Various rules (e.g. Plastic potential surface ≠ yield surface, and/or influenced by load increment direction)

Extras:

- **Yield surface**: Separates elastic from elastoplastic behaviour
- **Stress-dilatancy relationship**: volumetric expansion versus stress
- **Shear stress-vs-plastic shear strain**

Elastic model

Hyperelastic vs Hypoelastic formulation

Hypoelastic - non thermodynamically conservative elastic response

Hyperelastic - conservative

Hyperelastic formulation (Houlsby et al. (2005) - taken from Whyte 2020)

$$\begin{bmatrix} \delta\varepsilon_{vol} \\ \delta\varepsilon_q \end{bmatrix} = \begin{bmatrix} \frac{1}{K_{ref}(1-n)p_{ref}^{1-n}p_0^n}\left[1-\frac{np^2}{p_0^2}\right] & \frac{npq}{3G_{ref}p_{ref}^{1-n}p_0^{n+2}} \\ \frac{npq}{3G_{ref}p_{ref}^{1-n}p_0^{n+2}} & \frac{1}{3G_{ref}p_{ref}^{1-n}p_0^n}\left[1-\frac{nk(1-n)q^2}{3G_{ref}p_0^2}\right] \end{bmatrix} \begin{bmatrix} \delta p' \\ \delta q \end{bmatrix}$$

Note the coupling terms in the elastic stiffness matrix - causes stress-induced ansiotropy which is observed in experiments.

Common Hypoelastic formulation (e.g. Manzari and Dafalias (2005) - taken from Whyte 2020)

$$\begin{bmatrix} \delta\varepsilon_{vol} \\ \delta\varepsilon_q \end{bmatrix} = \begin{bmatrix} \frac{1}{K_{ref}\,F(e)p_{ref}\left(\frac{p'}{p_{ref}}\right)^n} & 0 \\ 0 & \frac{1}{3G_{ref}\,F(e)p_{ref}\left(\frac{p'}{p_{ref}}\right)^n} \end{bmatrix} \begin{bmatrix} \delta p' \\ \delta q \end{bmatrix} \qquad 2.14$$

Constant poissons ratio

Poissons ratio is dependent on density and confining pressure (Kumar et al. 2010)

Extended elastic model

Extended models have stress and/or strain dependent elasticity (e.g. based on G/G0 and Masing Rules)

Hardening/Softening rules

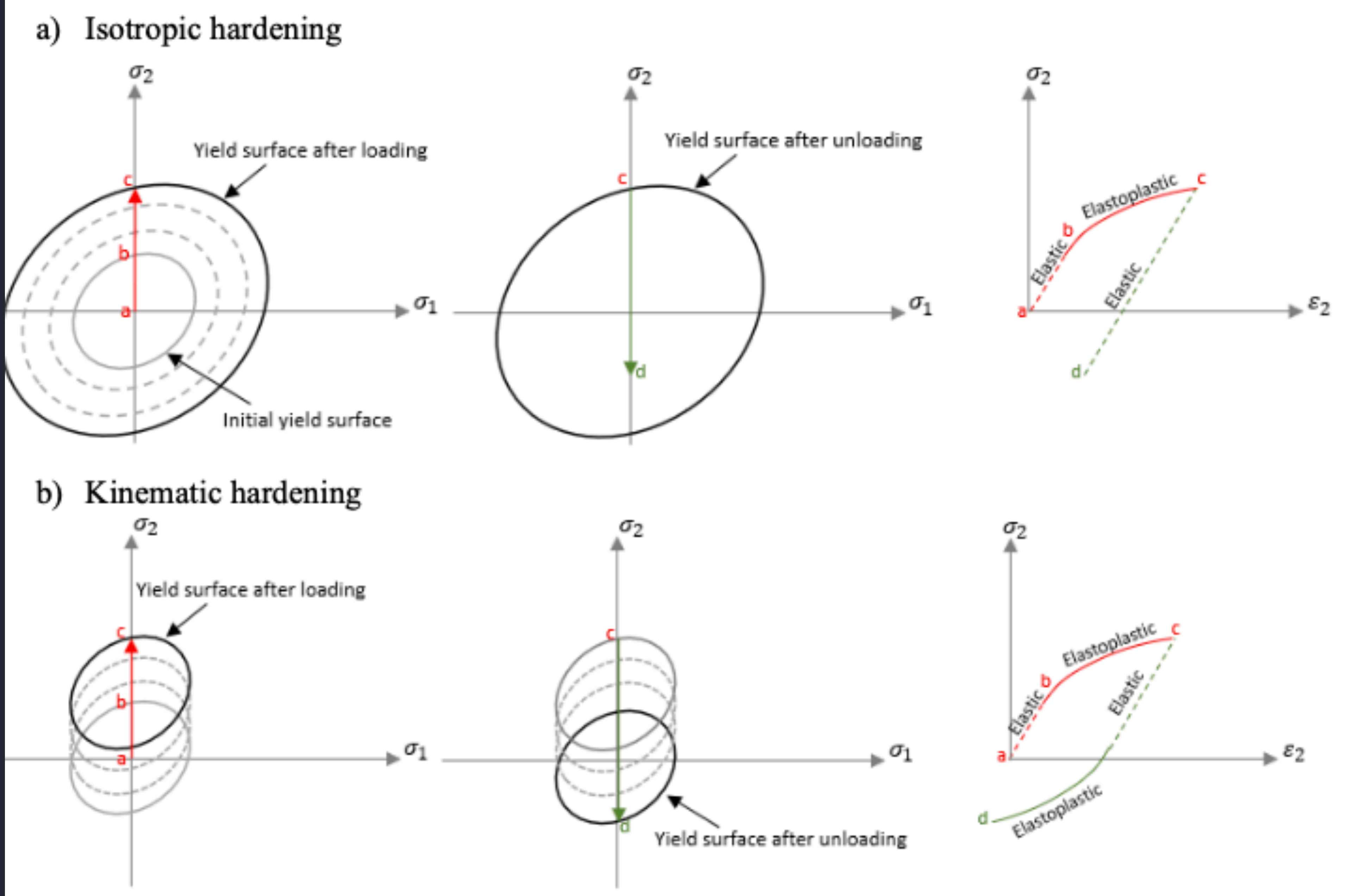

Figure 2.7: yield surface expansion/translation and stress-strain response for load-unload stress path for a) isotropic hardening model b) kinematic hardening model

Note: Using only a single isotropic hardening surface is only suitable for monotonic loading - not cyclic/unloading

Flow rule

Simple rule: e.g. associative flow rule in the MCC model, or fixed dilation angle.

Or complex pressure, strain, work, dilation and/or state dependent rules using stress-dilatancy relationships and stress-vs-plastic-shear-strain relationships.

can get very complex…

Note that problems with greater kinematic constraint are more sensitive to dilation (e.g. axially loaded piles versus slope stability) (Houlsby, 1991)

Associative flow rule

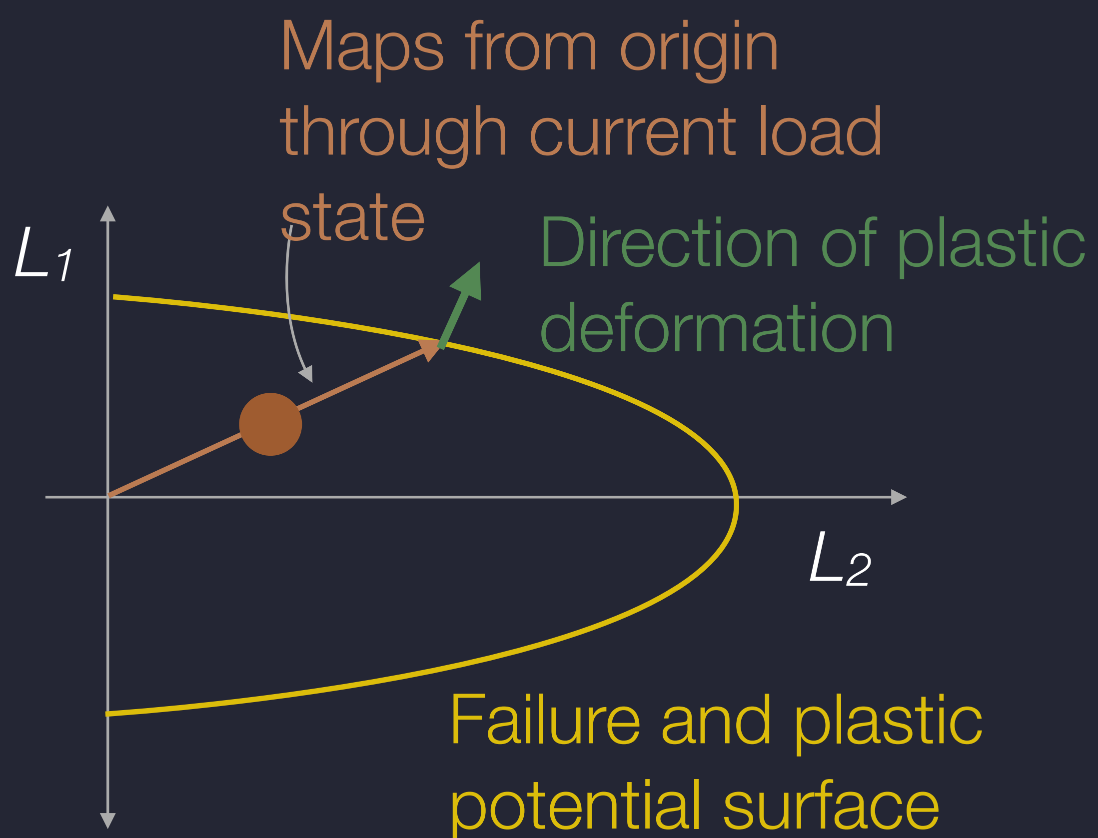

Arbitrary non-associative flow rule

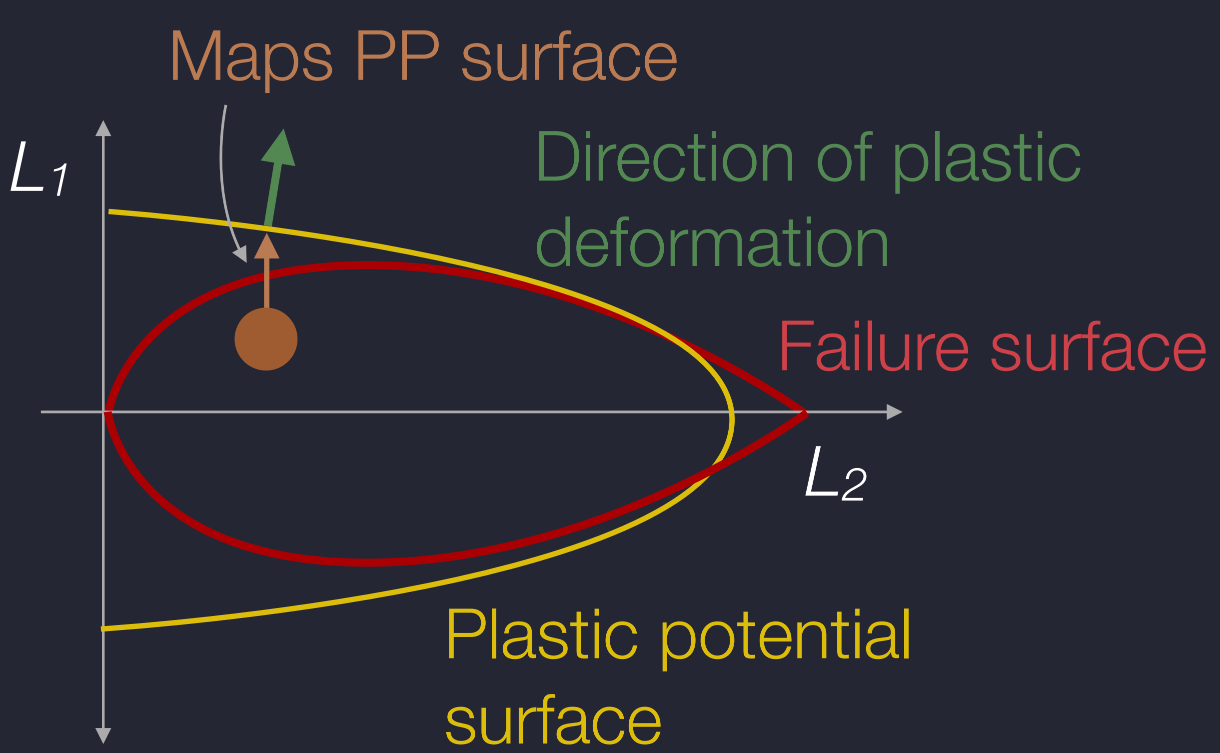

Stress-dilatancy: Friction angle and dilation

Simple saw tooth model 'theory'

(adapted from Houlsby 1991)

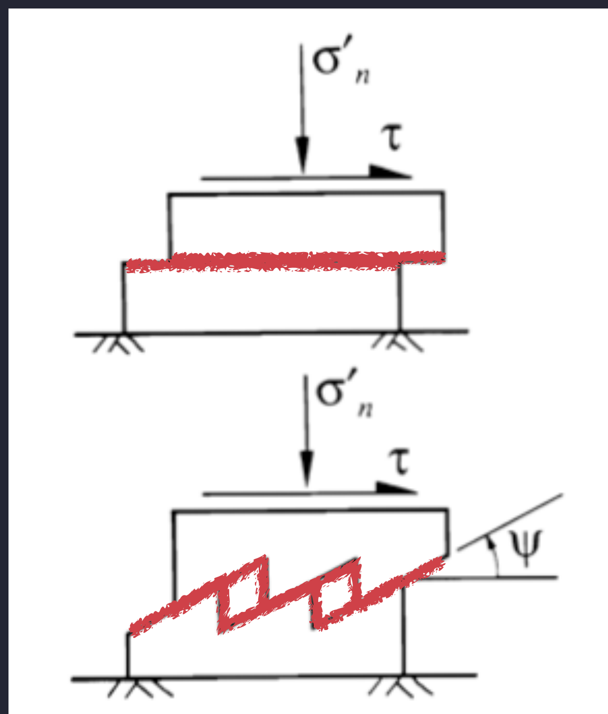

Figure 6, The sawtooth model for dilatancy

Friction stress under constant volume

$$\frac{\tau}{\sigma_n} = \tan\phi_{cv}$$

Friction stress with dilative behaviour

horizontal stress required to slide increases due to geometry of teeth

$$\frac{\tau}{\sigma_n} = \tan(\phi_{cv} + \psi)$$

Energy-based theory from Taylor (1948)

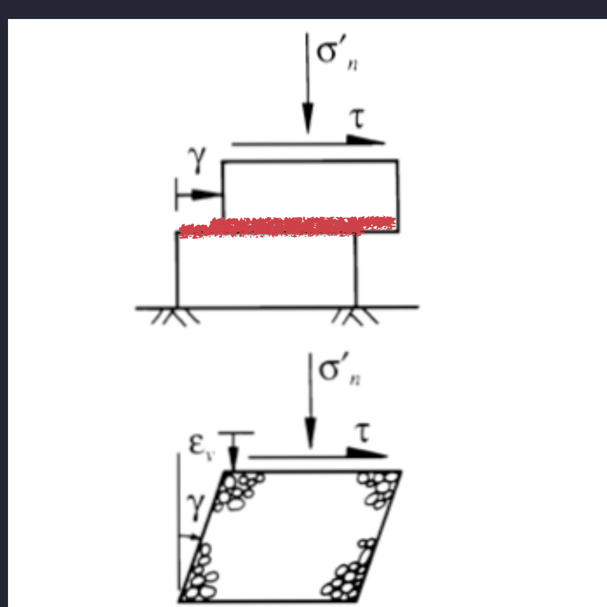

Figure 7, Analogy used in Taylor's energy correction

Friction work under constant volume

Theory assumes energy dissipated internal according to:

$$\dot{W} = \tau\dot{\gamma} = (\tan\phi_{cv})\sigma_n\dot{\gamma} \rightarrow \frac{\tau}{\sigma_n} = \tan\phi_{cv}$$

Friction work with dilative behaviour

Work from volumetric expansion

$$\dot{W} = \tau\dot{\gamma} + \sigma_n\dot{\epsilon}_v = (\tan\phi_{cv})\sigma_n\dot{\gamma} \rightarrow \frac{\tau}{\sigma_n} = \tan\phi_{cv} + \tan\psi$$

Rowe's (1962) stress-dilatancy theory

Simplified - original formulation was in terms of spheres.

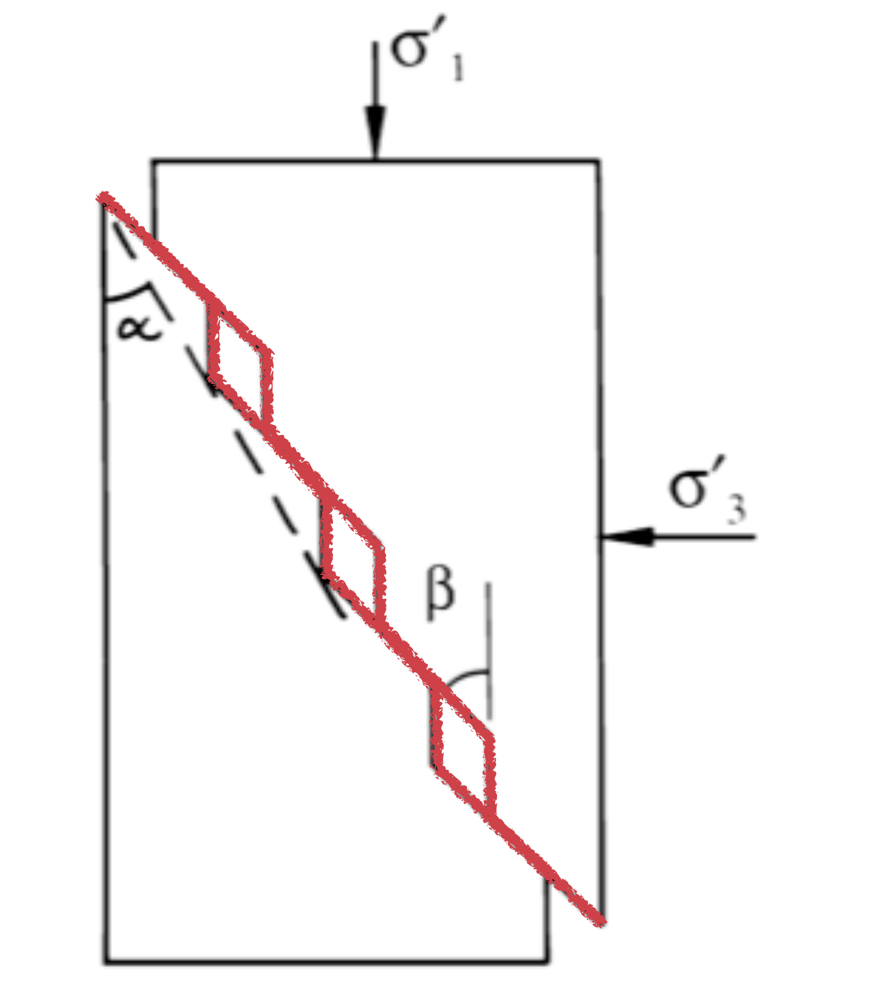

Figure 9, Assumed sliding mechanism for Rowe's stress-dilatancy flow rule

Formulated the problem in terms of principle stresses

$$\frac{\sigma_1}{\sigma_3} = \frac{\tan(\phi_\mu + \beta)}{\tan\beta} \cdot \frac{-\dot{\epsilon}_3}{\dot{\epsilon}_1}$$

Solve for minimum energy (or minimum stress):

$$\frac{\sigma_1}{\sigma_3} = \tan^2\left(\frac{\phi_\mu}{2} + \frac{\pi}{4}\right) \cdot \frac{-\dot{\epsilon}_3}{\dot{\epsilon}_1}$$

ϕ_μ Could be interpreted as ϕ_{cv} and grain-to-grain contact [not back by experimental evidence]

Note: used in DM04 model

Stress-dilatancy to pressure-density

Taken from Houlsby (1991)

Small reduction in normalised peak response with increasing σ

Steel balls all approach same void ratio

Peak strength dependent on density and pressure

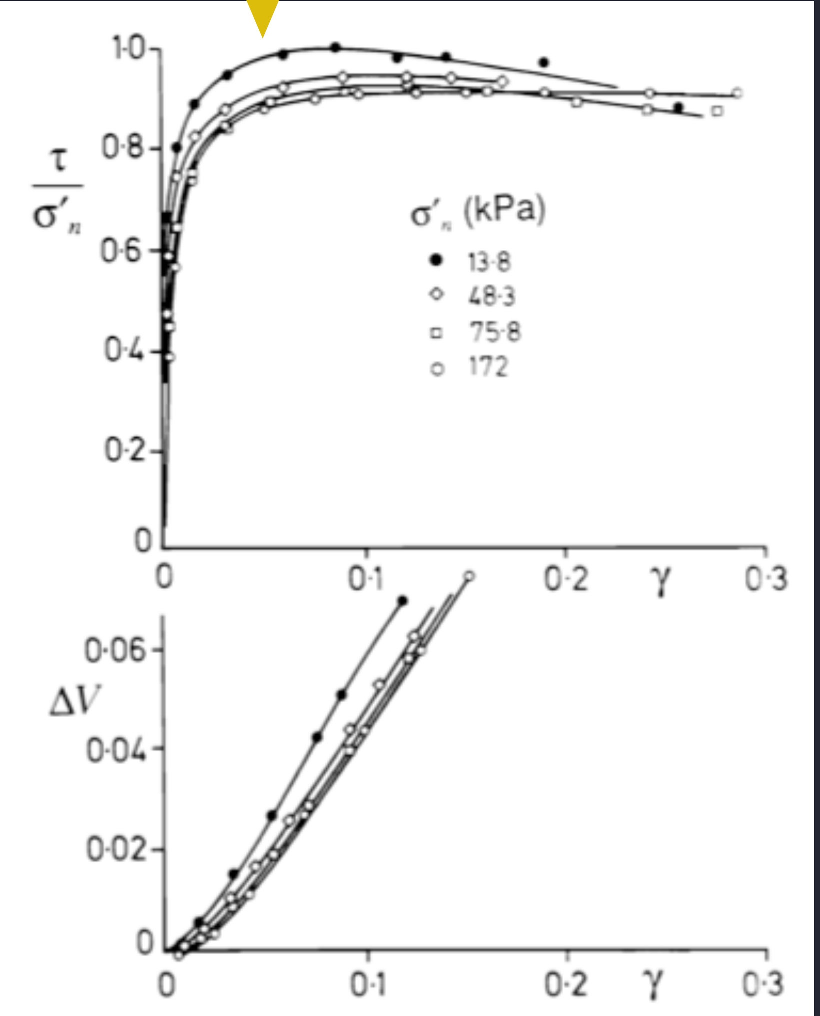

Figure 12, Shear stress - shear strain and volumetric strain - shear strain for simple shear tests on sand (after Stroud, 1971)

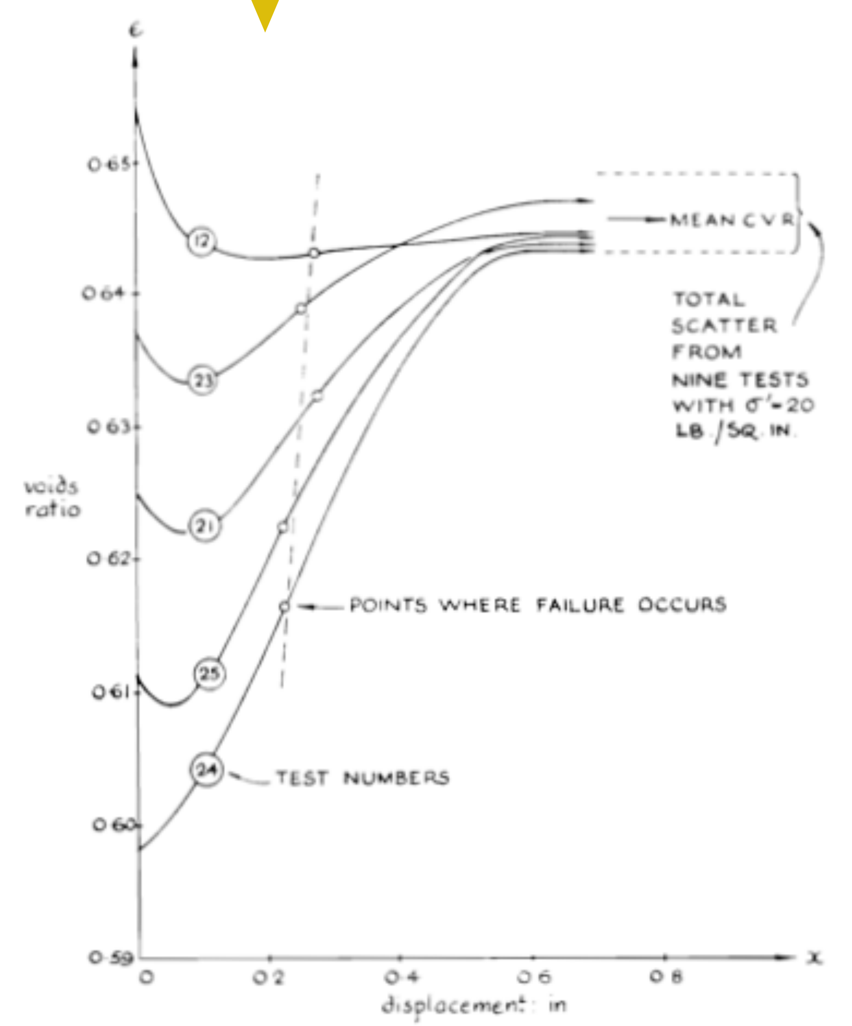

Figure 13, Voids ratio against shear displacement for simple shear tests on steel balls (from Wroth, 1958)

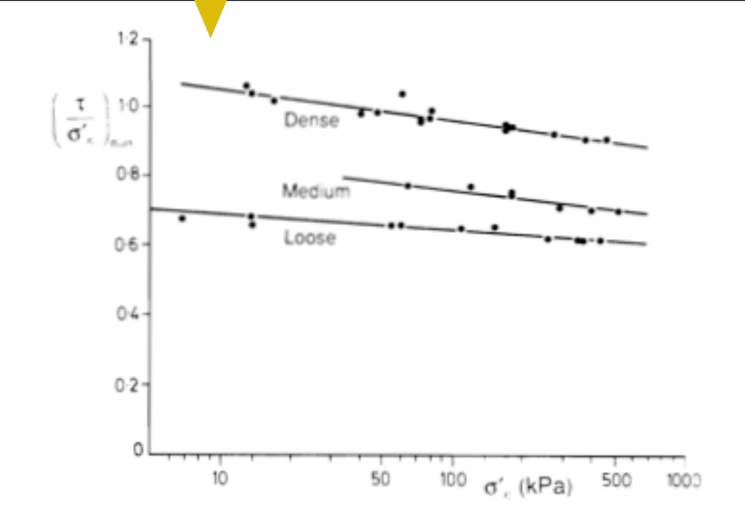

Figure 15, Peak strength against stress level for simple shear tests at different densities (after Stroud, 1971)

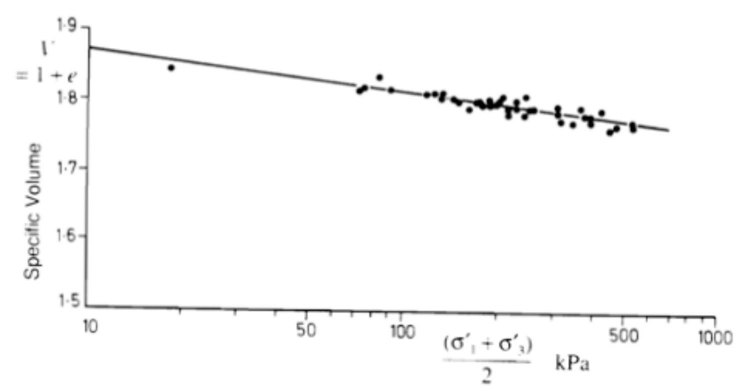

Figure 14, Critical State Line for simple shear tests on sand (after Stroud, 1971)

Critical specific volume (void ratio) dependent on pressure

Wroth's expression defined in terms of relative density as:

$$\sin\psi = A + B \cdot D_r - C \cdot ln\left(\frac{p'}{p_{atm}}\right)$$

Bolton’s (1986) stress-dilatancy relationship

Note: Bolton (1986) dilatancy relationship (used in PM4Sand) is an extension of Rowe’s model - but largely empirically based on experimental data.

$$\phi_p = \phi_{cv} + 0.8\psi_{\max}$$

Also empirically derived the peak friction angle:

$$\phi_p = \phi_{cv} + 5(D_r[Q - ln(\frac{p'}{p_{atm}})] - R)$$

For Q=10, R=1

$$\psi = -0.11 + 0.59D_r - 0.11D_r \cdot ln\left(\frac{p'}{p_{atm}}\right)$$

Rules are similar but different…

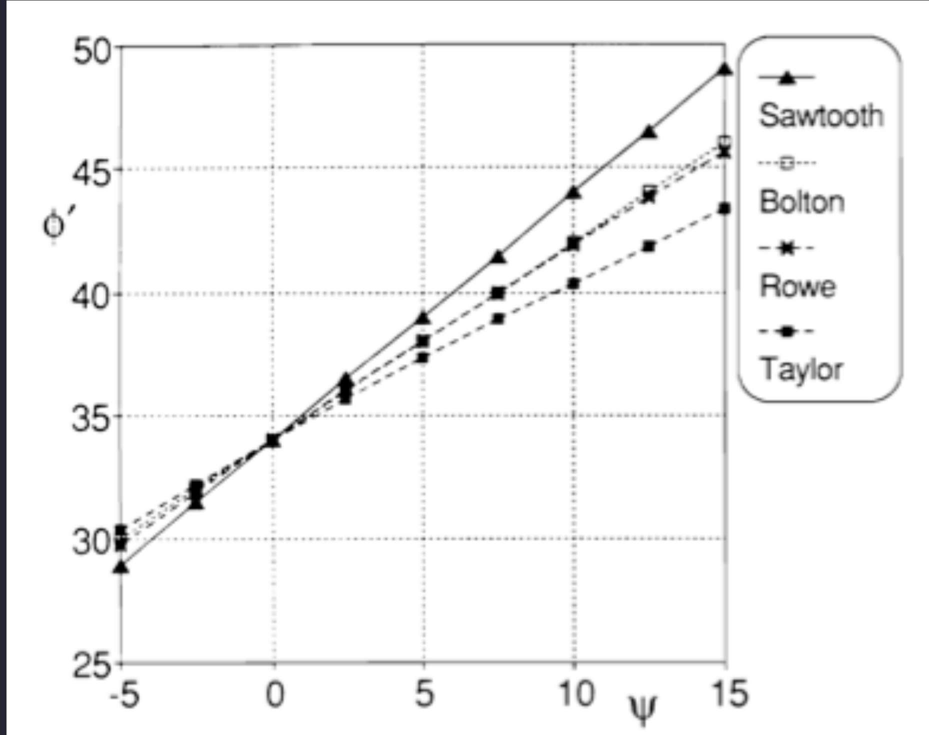

Figure 10, Comparison of flow rules

Stress-vs-plastic strain: Failure in triaxial space

Main issue for 3D behaviour is that ϕ_{cv} is different for different modes of shearing, e.g. larger for TXC than TXE.

Houlsby (1991) provides a work-based hypothesis to address this

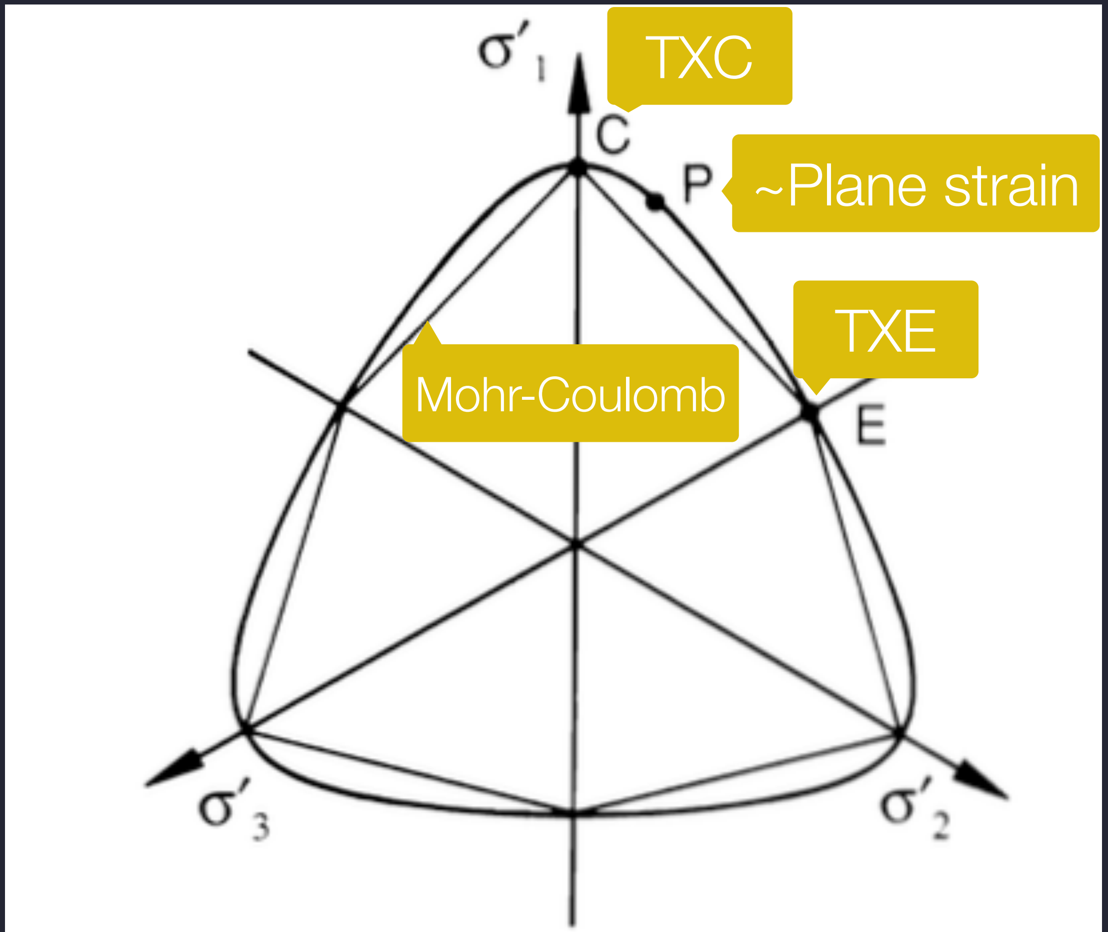

Figure 35, Matsuoka's failure criterion in the octahedral plane

The majority of models employ a Lode angle relationship θ to adjust M or ϕ based on σ_2

Note: the Lode angle relationship depends on failure surface (e.g. Matsuoka 1976, Lade 1975)

Common yield surface shapes

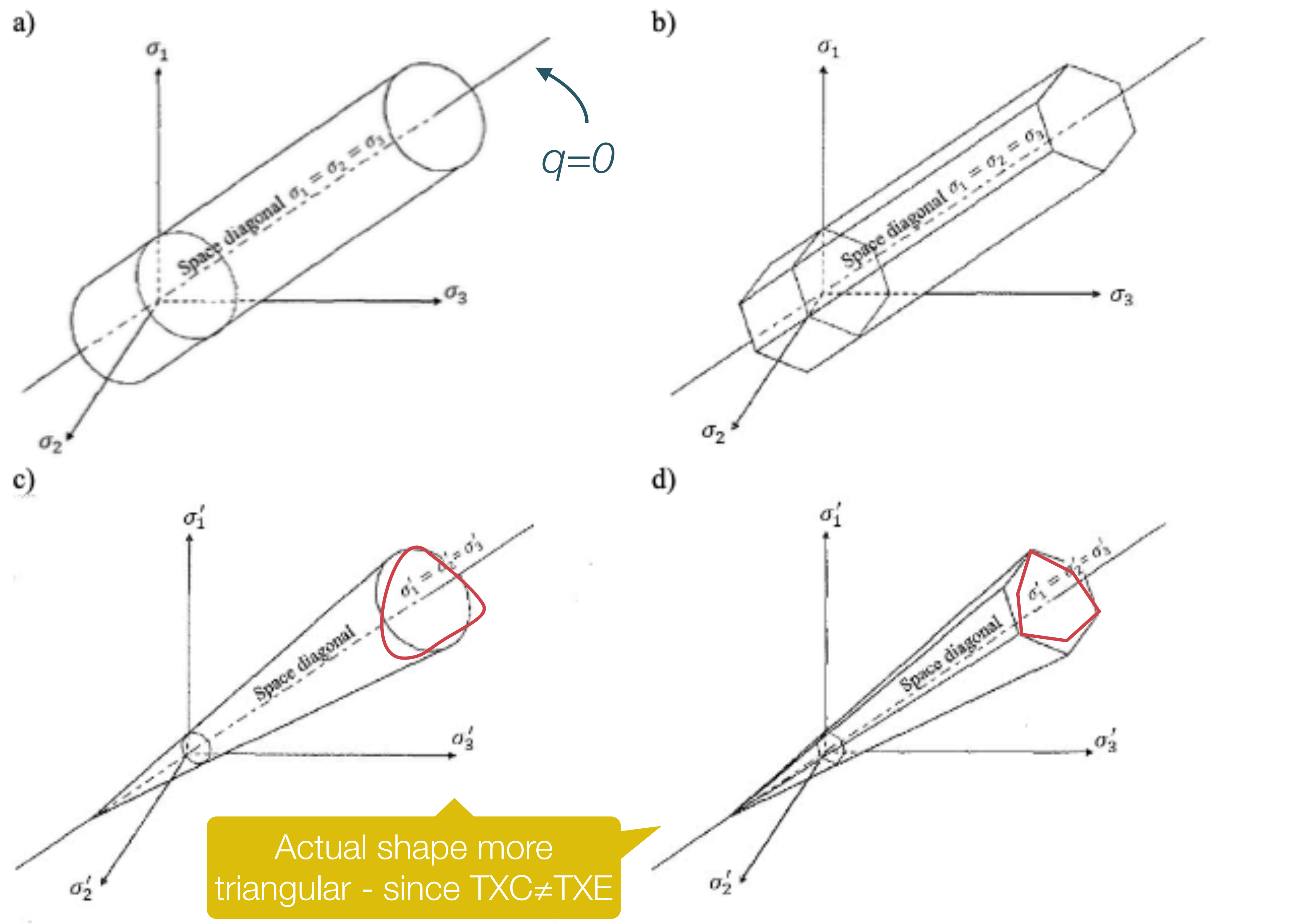

Figure 2.5: Total stress yield surfaces a) von Mises and b) Tresca and effective stress yield surfaces c) Drucker-Prager d) Mohr-Coulomb (after. Potts and Zdravković, 1999)

Available soil models

36 papers on new soil models or calibrations at the NUMGE 2018 Conference

- Reviewing only widely used and implemented within widely available software
- Pure non-cementitious soil
- Not comprehensive

Family Tree

Only 2D formulation

Manzari & Dafalias (1997)

Li and Dafalias (2000)

DM04/ SANISAND04: Dafalias & Manzari (2004) [OpenSees]

Overshoot correction, nonlinear isotropic

SANISAND: Taiebat & Dafalias (2008) [FLAC3D]

SANICLAY: Seidalinov & Taiebat (2014) - other extensions

Modified for clay-like material

SANISAND-Z: Dafalias & Taiebat (2016)

No yield surface, load increment mapping rule

SANISAND-MSf: Yang, Taiebat & Dafalias (2020)

Added memory surface and fluidised state for strain rate post-liq

SANISAND-MS: Liu et al. (2020) [OpenSees]

Added memory surface for controlling rate of strain under constant cyclic amplitude

PM4Sand v3.1: Boulanger and Ziotopolous (2017) [FLAC2D, OpenSees, PLAXIS]

PM4Silt: Boulanger and Ziotopolous (2018) [FLAC2D, OpenSees, PLAXIS]

NTUA: Adrainopoulos et al. (2010) [FLAC2D]

Nor-Sand (Jefferies 1993) → **Nor-Sand (3D)** (Chen and Jefferies 2000) [FLAC3D, PLAXIS]

SD-model: Cubrinovski and Ishihara (1998) [Dyna,FLAC2D, OpenSees]

Other models not investigated:

- Popescu and Prevost (1993) [DYNAFLOW]
- Loukidis and Salgado (2009)
- Ling and Yang (2006)
- Andrade and Borja (2006)
- Zhang and Wang (2012)
- Petalas et al. (2019)

To understand a child … look at its parents!

DM04: DafaliasManazari model (2004)

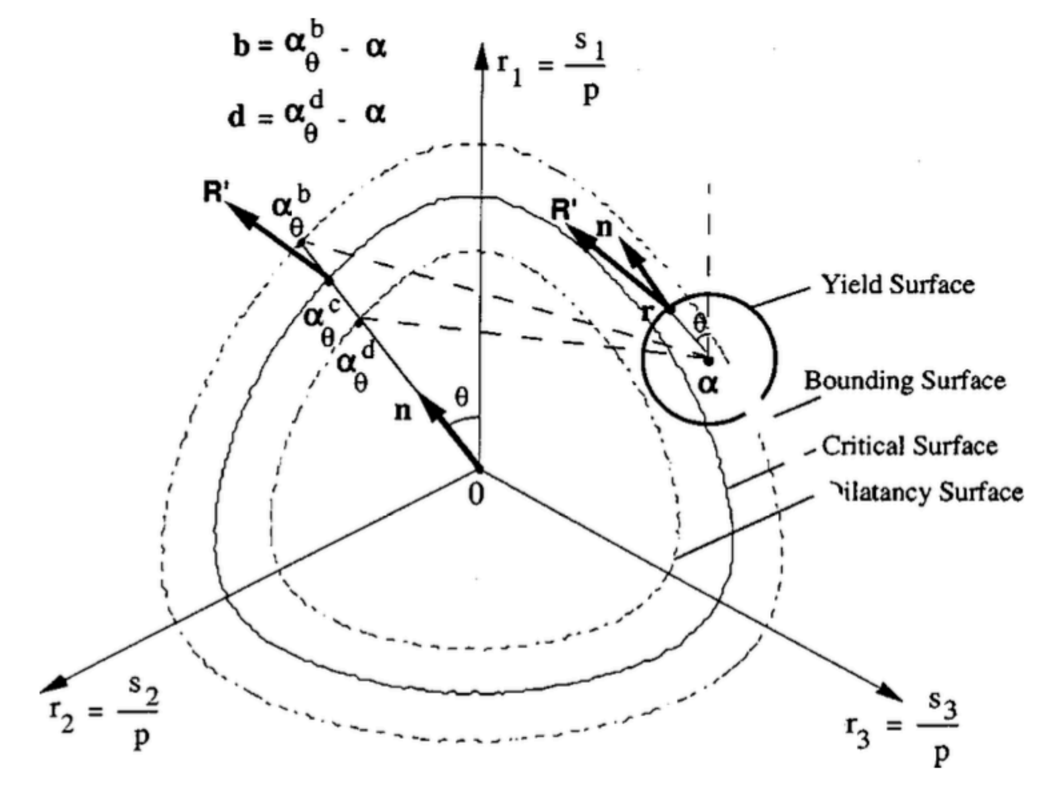

Fig. 4. Schematic of yield, critical, dilatancy, and bounding surfaces on the stress ratio π plane

- Flow rules governed by bounding surface model:
  - Bounding surface
  - Critical surface
  - Dilatancy surface
- Has a yield surface
- State parameter controls position of bounding and dilatancy surfaces
- Fabric change controlled by volumetric expansion

<u>Some issues with DM04:</u>

- Overshooting (after small unload/reload)
- Elastic response under isotropic loading
- Strain locking at liquefied state
- Excessive strain under repeated cycles (dry)
- Typically calibrated with low Poisson's ratio (0.05)

PM4Sand

- Reformulated in terms of relative density
- Uses adaption of Bolton's dilatancy relationship
- Only plane strain
- Models post-liquefaction cyclic behaviour
- Improved control of contraction rate
- Improved dilatancy using a rotated dilatancy surface (earlier dilatancy if stress reversal)
- Overshooting correction

Read DM04 to understand PM4Sand

Comparison - Elastic model

SD-model

Elastic shear modulus:

$$G = A \cdot p_{atm} \frac{(2.17 - e)^2}{1 + e} \left(\frac{p}{p_{atm}} \right)^n$$

Elastic bulk modulus:

$$K = \frac{2(1 + \nu)}{3(1 - 2\nu)}$$

Isotropic elastic formulation

No yield surface

DM04-model

Elastic shear modulus:

$$G = G_0 \cdot p_{atm} \frac{(2.97 - e)^2}{1 + e} \left(\frac{p}{p_{atm}} \right)^{0.5}$$

$$K = \frac{2(1 + \nu)}{3(1 - 2\nu)}$$

Isotropic elastic formulation

Kinematic cone yield surface

$A \leftrightarrow G_0$

Both use constant ν

Comparison - Plastic shear strain relationship

SD-model

$$\frac{q}{p} = \frac{G_N \varepsilon_q^p \left(\frac{q}{p}\right)_{max}}{\left(\frac{q}{p}\right)_{max} + G_N \varepsilon_q^p}$$

$$H_p = \left\{ G_N - f \frac{\varepsilon_q^p}{0.01} (G_N - G_{N,min}) \right\} p \left\{ 1 - \frac{\eta}{\eta_{max}} \right\}^2 \quad (35)$$

$$\left(\frac{q}{p}\right)_{max} = a_1 + b_1 I_s$$

Note: G_N is dependent on state

$$G_{N,\max} = a_2 + b_2 I_s$$

$$G_{N,\min} = a_3 + b_3 I_s$$

$$G_N = (G_{N,\max} - G_{N,\min}) \cdot \exp\left(-f \frac{\epsilon_q^p}{\epsilon_q^0}\right) + G_{N,\min}$$

Note: G_N degrades with amplitude of strain

Plane strain wedge (q/p) failure surface

Modified hyperbolic vs Bounding surface formulation

$$\left(\frac{q}{p}\right)_{max} \leftrightarrow M_b$$

$$G_N \leftrightarrow b_0$$

DM04-model

$$d\varepsilon_q^p = \frac{d\eta}{H}; \quad H = h(M^b - \eta) \quad h = \frac{b_0}{|\eta - \eta_{in}|};$$

$$\frac{d\eta}{d\epsilon_p^q} = \frac{b_0(M_b - \eta)}{|\eta - \eta_{in}|}$$

Note: No strain in tangent stiffness

$$M_b = M \exp(-n^b \psi) = \eta_b$$

Note: b_0 is dependent on e, G_0, p'

$$b_0 = G_0 h_0 (1 - c_h e)(p/p_{atm})^{-0.5}$$

Note: in later formulations (e.g. PM4Sand) G_0 degrades with cumulative strain

2D wedge, 3D cone (q/p) failure surface with Lode angle where Qe/Qc ratio is an input

Comparison - Stress-dilatancy relationship

$$d\epsilon_v^p / d\gamma_p = f$$

SD-model

Stress-Dilatancy Relation

The stress-dilatancy relation is based on the energy approach (Roscoe et al., 1963) and is given by

$$\frac{d\varepsilon_v^p}{d\varepsilon_q^p} = \mu - \frac{q}{p} c \qquad (7)$$

Based on dissipated energy (Roscoe 1963)

$$\mu = \frac{\left(\frac{dW}{p}\right)}{d\varepsilon_q^p} = \frac{d\Omega}{d\varepsilon_q^p}$$

Empirically based on experimental evidence

$$\mu = \mu_0 + \frac{2}{\pi}(M - \mu_0)\tan^{-1}\left(\frac{\varepsilon_q^p}{S_c}\right) \qquad (11)$$

Co-axiality term:

$$c_{SD} = \cos(2\psi_{SD})$$

Different to c and ψ from DM04 model

ψ_{SD} is the angle between the principle stress and the direction of the plastic strain increment

$$\mu \leftrightarrow M_d$$

DM04-model

$$d\varepsilon_v^p = d\left|d\varepsilon_q^p\right| \qquad (2)$$

$$d = A_d(M^d - \eta) \qquad (7)$$

$$M^d = M \exp(n^d \Psi) \qquad (10)$$

Based on Rowe's (1962) theory

Note: μ0 is the slope of normalised <u>shear</u> work vs plastic shear strain

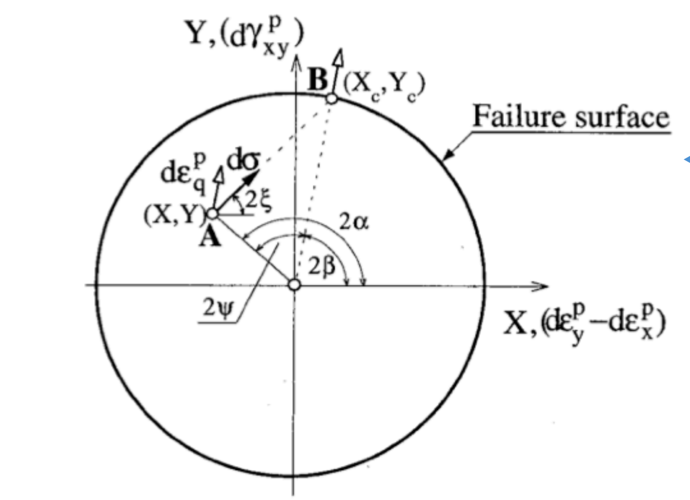

Fig. 6. Flow rule (Gutierrez et al., 1993)

Mapping rule based on load increment

Comparison - Other aspects

- Unload-reload handle through tracking multiple load surfaces in SD vs back stress ratios for Mb and Md in DM04.
- SD uses State Index vs State Parameter in DM04 to quantify soil state
- Both require only a single set of parameters for all densities and pressures
- Note: DM04 often calibrated with Poisson’s ratio of 0.05 - since open wedge/cone yield surface

Advice

"The art of soil modelling thus lies in being able to identify important characteristics while leaving the model as simple as possible.... There is a law of diminishing returns as attempts are made to use progressively more sophisticated – and hence potentially more realistic (?) – models for design and analysis." Wood (1991)

My advice: Validate your model at both the element level and system level under all relevant load paths

References

Cheng, Z. & Jefferies, M. Implementation and Verification of NorSand Model in General 3D Framework. *Geo-congress 2020* 10–19 (2020)

Cubrinovski, M. & Ishihara, K. MODELLING OF SAND BEHAVIOUR BASED ON STATE CONCEPT. *Soils and foundations* **38**, 115–127 (1998).

Cubrinovski, M. & Ishihara, K. State concept and modified elastoplasticity for sand modelling. *Soil and Foundations* 1–13 (1998).

Jefferies, M. G. Nor-Sand: a simple critical state model for sand. *Géotechnique* **43**, 91–103 (1993).

KUMAR, J. & MADHUSUDHAN, B. N. Effect of relative density and confining pressure on Poisson ratio from bender and extender elements tests. *Géotechnique* **60**, 561–567 (2015).

Ling, H. I. & Yang, S. Unified Sand Model Based on the Critical State and Generalized Plasticity. *Journal of Engineering Mechanics* **132**, 1380–1391 (2006).

Loukidis, D. & Salgado, R. Modeling sand response using two-surface plasticity. *Computers and Geotechnics* **36**, 166–186 (2009).

Prevost, J. H. & Popescu, R. Constitutive relations for soil materials. *The Electronic Journal of Geotechnical Engineering* (1996).

Whyte S. A. Development, Implementation, Calibrationand Use of Practical Constitutive Models in Finite Element Analysis of Offshore Foundations (2020)

QuakeCore 2 - Future Research Ideas

Liquefaction triggering - 3D liquefaction resistance

Bi-directional loading:

Why: We know that out-of-plane loading influences PP build up but we don't account for it in assessment

Experiment (Kammerer et al. 2002)

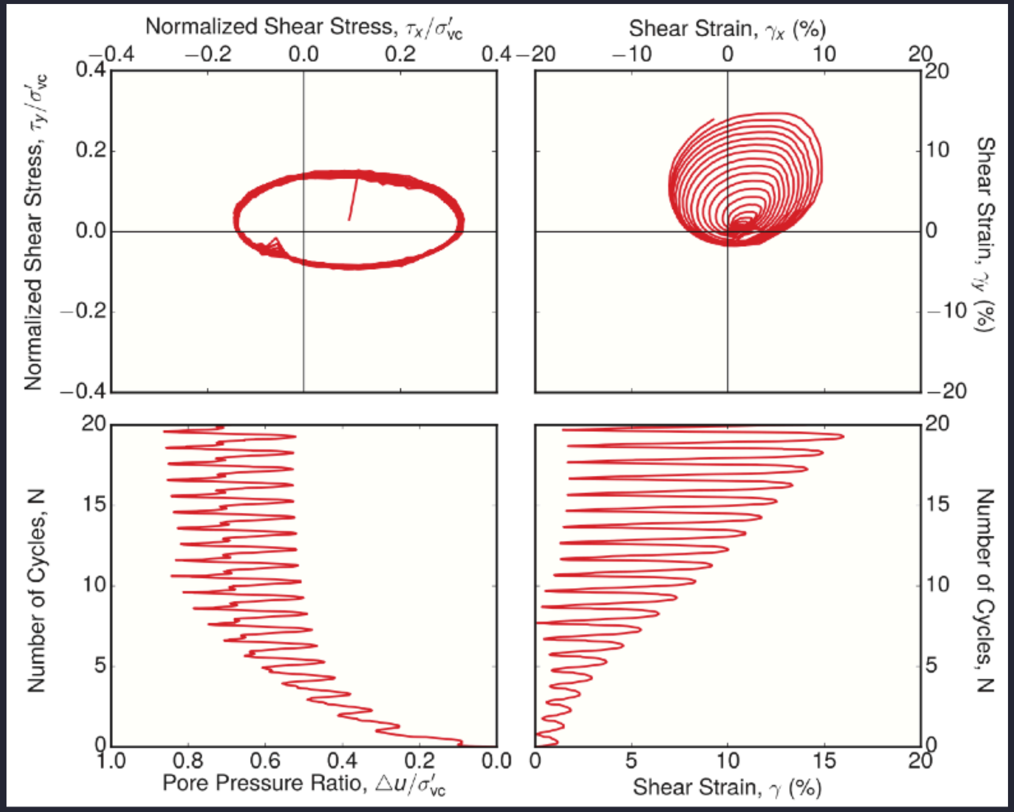

Simulation (Yang et al. 2018)

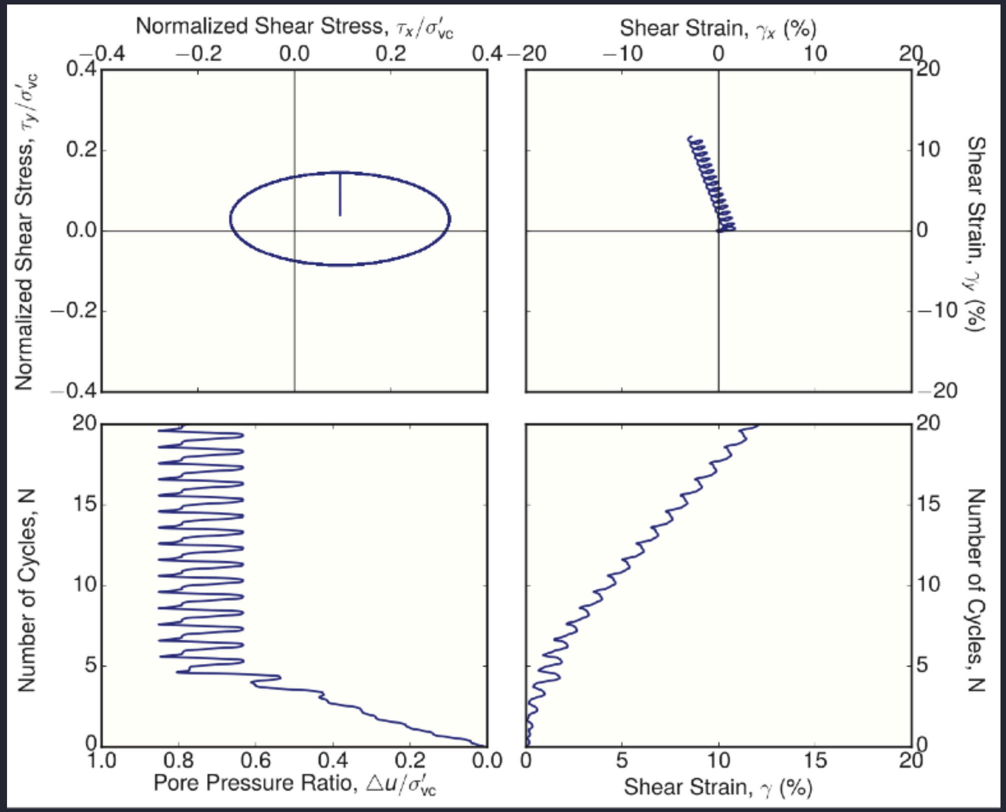

- Quantify influence of bi-directional GM (and GM directivity)
- Quantify out-of-plane static shear stress on resistance (e.g. LS problems)
- Improved simulation

How: Field case histories, DEM, Laboratory testing, 3D FEM

Kammerer AM, Pestana JM, Seed RB. Undrained response of monterey 0/30 sand under multidirectional cyclic simple shear loading conditions, Geotechnical Engieering Report UCB/GT/02-01, University of California, Berkeley (July 2002).

*Yang, M., Seidalinov, G. & Taiebat, M. Multidirectional cyclic shearing of clays and sands Evaluation of two bounding surface plasticity models. Soil Dynamics and Earthquake Engineering **124**, 1–29 (2018).*

Liquefaction triggering - 3D liquefaction demand

Bi-directional loading:

Why: Current assessment procedures using geometric mean PGA - PP is driven by cumulative strain.

State-of-the-art/practice:

- Seed et al. (1975) Cycle counting procedure does not account for out-of-plane loading.
- Bi-directional loading tests show load path influences PP build up not just peaks (Kammerer et al 2002)
- Cumulative intensity measures (e.g. Arias Intensity, CAV, cumulative strain energy) have strong correlation to PP build up (Dashti & Karimi 2007, Millen et al. 2020)

Contributions:

- Improve estimation of equivalent CSR using additional IMs
- Improve estimation of equivalent CSR accounting for out-of-plane GM loading
- Procedures/guidelines for effective stress analysis & GM selection

How: Field case histories, 2D/3D FEM

Dashti, S. & Karimi, Z. Ground Motion Intensity Measures to Evaluate I: The Liquefaction Hazard in the Vicinity of Shallow-Founded Structures. *Earthquake Spectra* **33**, 241–276 (2017).

Millen, M. D. L., Rios, S., Quintero, J. & Fonseca, A. V. da. Prediction of time of liquefaction using kinetic and strain energy. *Soil Dynamics and Earthquake Engineering* **128**, 105898 (2020).

Liquefaction triggering - liquefaction demand with depth

Why: Current approaches rely on rigid body assumption, however, there are alternatives. Does not account for large impedance contrasts. Requires total stress equivalent motion.

State-of-the-art/practice:
Note figure normalised by PGA
1D equivalent linear analysis

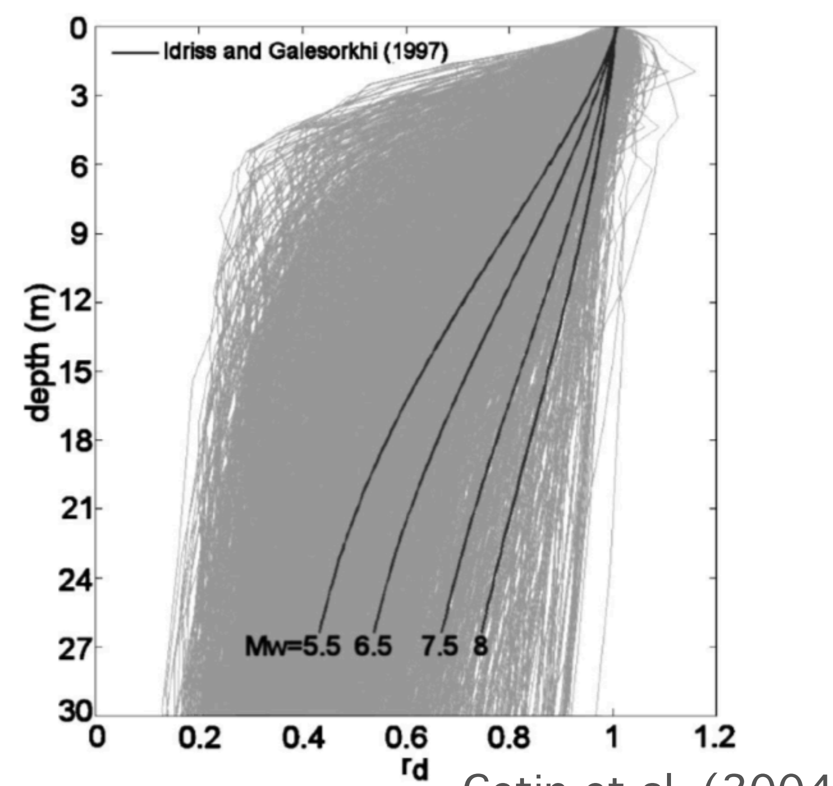

Cetin et al. (2004)

Fig. 5. Improved r_d recommendations of Idriss and Golesorkhi (personal communication, 1997) and comparison with calculated values from current study

Contributions:

- Improve estimation of equivalent CSR at depth

How: Field case histories, FEM

Cetin, K. O. *et al*. Standard Penetration Test-Based Probabilistic and Deterministic Assessment of Seismic Soil Liquefaction Potential. *Journal of Geotechnical and Geoenvironmental Engineering* **130**, 1314–1340 (2004).
Cubrinovski, M., Rhodes, A., Ntritsos, N. & Ballegooy, S. van. System response of liquefiable deposits. *Soil Dynamics and Earthquake Engineering* 1–18 (2018) doi:10.1016/j.soildyn.2018.05.013.

Liquefaction triggering - Energy-based approach

Why: Liquefaction is plastic strain controlled - therefore stress-based approaches are strongly dependent on stiffness. Alternative procedures emphasis different aspects of soil response

State-of-the-art/practice:

- Dissipated energy provides a load independent measure of liquefaction resistance (Davis and Berrill 1982, Kokusho 2013)
- Can either estimate demand through the total travelling wave energy (Davis and Berrill 1982, Kokusho 2013), or the cumulative strain energy in a layer (Millen et al. 2020)

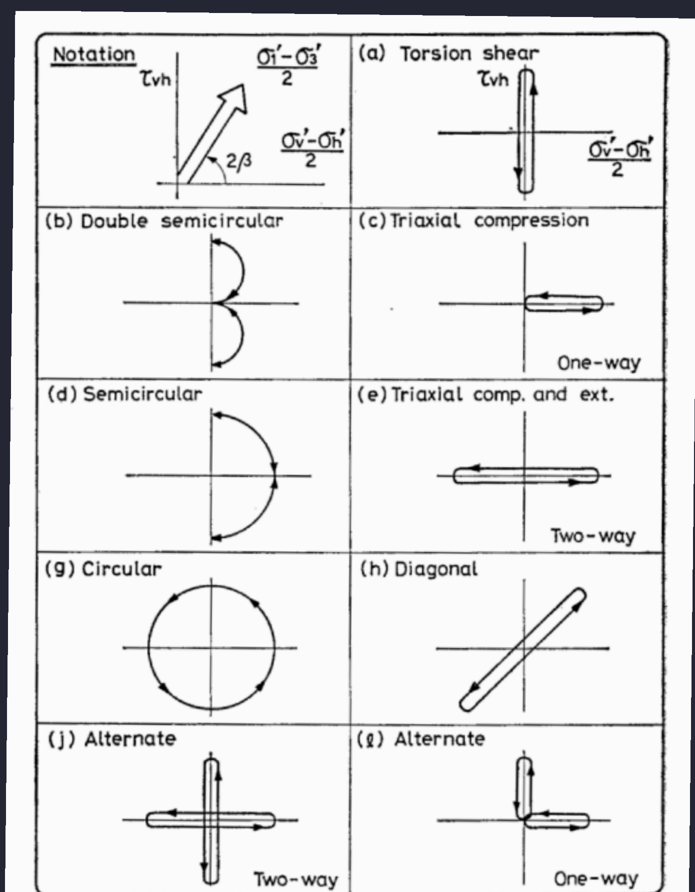

Fig. 2. Loading schemes used in this study

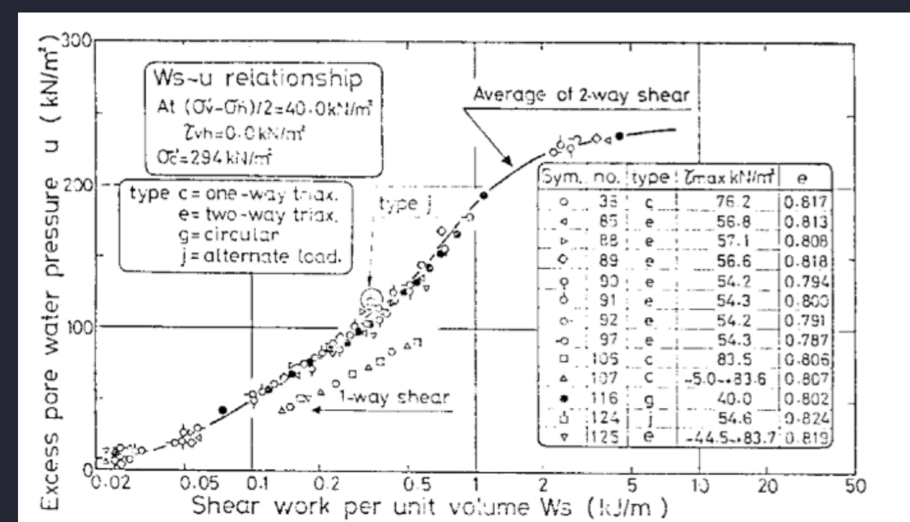

Fig. 18. Shear work correlation at triaxial compression of 40.0 kN/m²

Additional laboratory evidence:

- Nemat-Nasser & Shokooh (1979)
- Green et al. (2000)
- Kokusho (2013)
- Azeiteiro et al. (2013)

Energy based approaches provide an alternative perspective

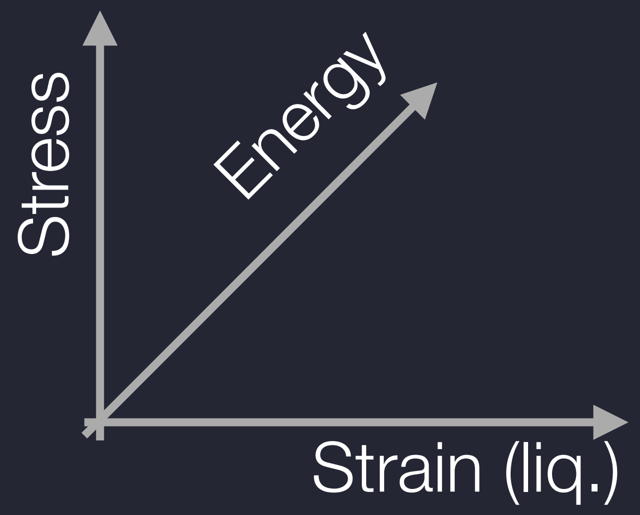

Rotate the problem by 45 degrees

Liquefaction triggering - Energy-based approach

Estimating strain from stress

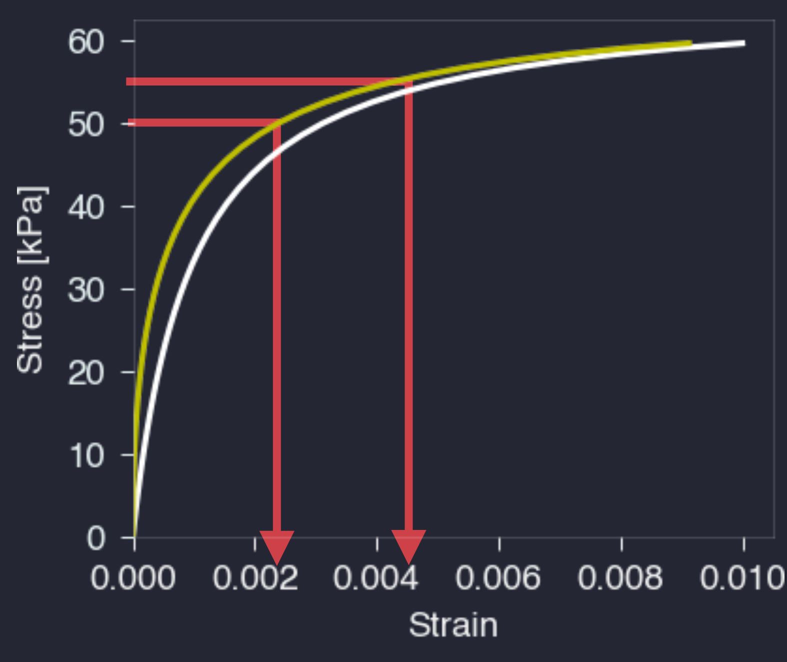

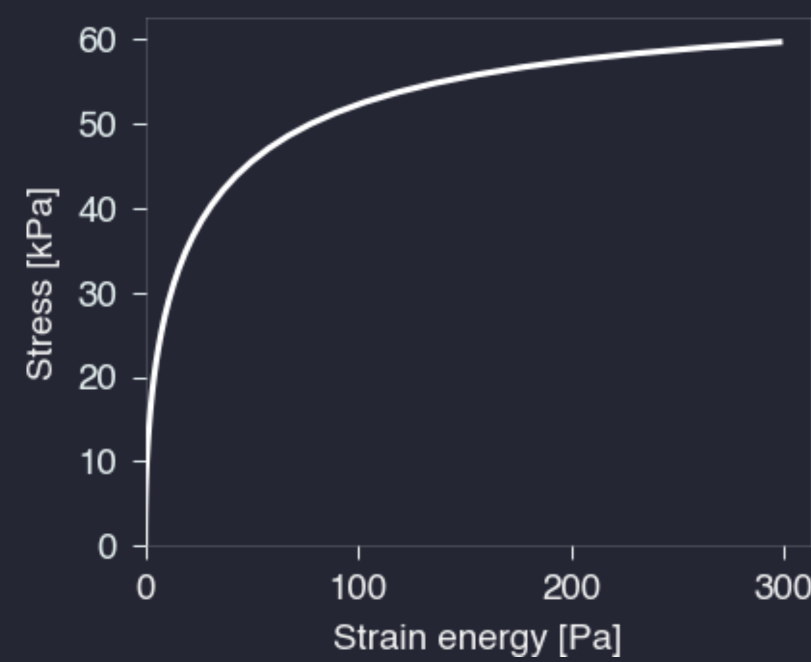

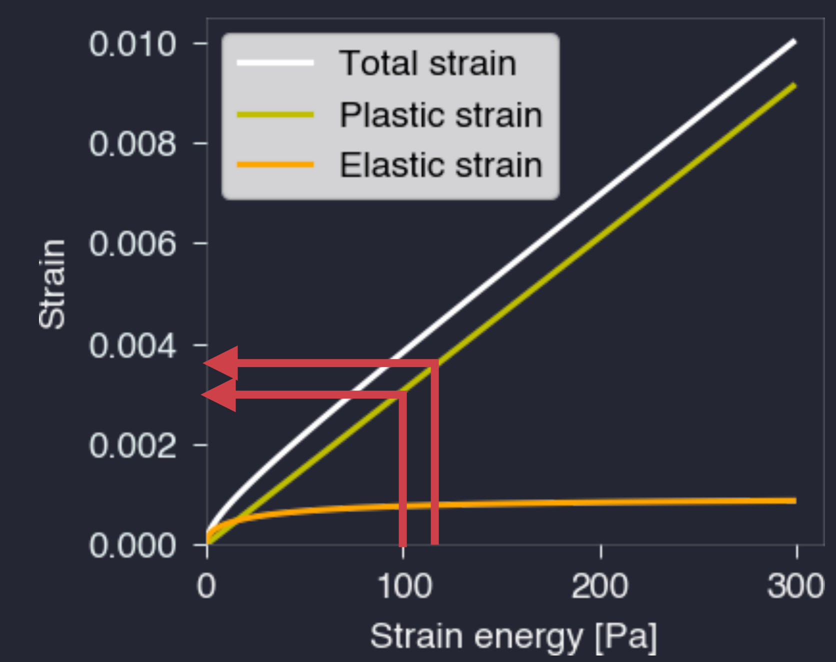

+10% Stress -> 45% strain

+10% Energy -> 10% strain

Contributions:

- Interpretation influence density, as well as fines and plasticity using an alternative perspective

How: Field case histories, laboratory testing, FEM

Kokusho, T. Liquefaction potential evaluations: energy-based method versus stress-based method. *Canadian Geotechnical Journal* **50**, 1088–1099 (2013).

Millen, M. D. L., Rios, S., Quintero, J. & Fonseca, A. V. da. Prediction of time of liquefaction using kinetic and strain energy. *Soil Dynamics and Earthquake Engineering* **128**, 105898 (2020).

Liquefaction & Buildings

- Load cases for considering soil variability under buildings (i.e. given 3 CPTs at a site (or geological enviro), how should engineer consider soil variability under building - stiffness/settlement/GMs)
- Naming conventions and handling of layers that change properties
- Guidance on combined GM loading (Pushover) and liquefaction effects (tilts/differential settlement) for seismic assessment
- Lateral spreading effects on shallow foundation buildings
- Influence of nearby buildings on liquefaction and building response [System level studies]

Other areas

- Re-liquefaction - Importance in understanding life-of-building/site risks/costs
  - DEM studies show importance of grain orientation and whether complete mobilisation is reached (Wang et al. 2016)
- Effectiveness of shear keys for mitigating lateral spreading and unstable slopes
- Improved liquefaction demand measures for ground motion selection
  - (i.e. IMs for triggering, LS, and settlement) (Karimi et al. 2017)
- Influence of partial liquefaction (ru<1) on buried infrastructure (e.g. uplift pressure and large deformations)
- Where possible QuakeCore could aim to provide consistent nomenclature for parameters across different studies.
- System-level response often doesn't have easily interpretable and generalisable trends - therefore research output should focus on providing modelling guidance

Wang, R., Fu, P., Zhang, J.-M., & Dafalias, Y. F. (2016). DEM study of fabric features governing undrained post-liquefaction shear deformation of sand. Acta Geotechnica, 11(6), 1321–1337. http://doi.org/10.1007/s11440-016-0499-8

*Karimi, Z., Spectra, S. D. E. & 2017. Ground motion intensity measures to evaluate II: The performance of shallow-founded structures on liquefiable ground. earthquakespectra.org **33**, 277–298 (2017).*